Tricarbonyl M(I) (M = Re, ^{99m}Tc) complexes bearing acridine fluorophores: synthesis, characterization, DNA interaction studies and nuclear targeting†

Teresa Esteves,[a] Catarina Xavier,‡[a] Sofia Gama,[a] Filipa Mendes,[a] Paula D. Raposinho,[a] Fernanda Marques,[a] António Paulo,[a] João Costa Pessoa,[b] José Rino,[c] Giampietro Viola§[d] and Isabel Santos*[a]

Received 3rd May 2010, Accepted 15th June 2010
First published as an Advance Article on the web 20th July 2010
DOI: 10.1039/c0ob00073f

New pyrazolyl-diamine ligands with acridine derivatives at the 4-position of the pyrazolyl ring were synthesized and characterized (**L1** and **L2**). Coordination towards the *fac*-$[M(CO)_3]^+$ (M = Re, ^{99m}Tc) led to complexes *fac*-$[M(CO)_3(\kappa^3\text{-L})]$ (L = **L1**: M = **Re1**, **Tc1**; L = **L2**: M = **Re2**, **Tc2**). The interaction of the novel pyrazolyl-diamine ligands (**L1** and **L2**) and rhenium(I) complexes (**Re1** and **Re2**) with calf thymus DNA (CT-DNA) was investigated by a variety of techniques, namely UV-visible, fluorescence spectroscopy and circular and linear dichroism. Compounds **L1** and **Re1** have moderate affinity to CT-DNA and bind to DNA by intercalation, while **L2** and **Re2** have a poor affinity for CT-DNA. Moreover, LD measurements showed that **L1** and **Re1** act as perfect intercalators. By confocal fluorescence microscopy we found that **L1** and **Re1** internalize and localize in the nucleus of B16F1 murine melanoma cells. The congener **Tc1** complex also targets the cell nucleus exhibiting a time-dependent cellular uptake and a fast and high nuclear internalization (67.2% of activity after 30 min). Plasmid DNA studies have shown that **Tc1** converts supercoiled (sc) puc19 DNA to the open circular (oc) form.

Introduction

Treatment of cancer still remains a great challenge for modern medicine, in particular the eradication of disseminated tumor cells and small metastases which cannot be treated efficiently with external radiation therapy or surgery. More recently, radionuclide therapy started to be envisaged as an alternative and powerful modality for the treatment of disseminated malignant diseases.[1] So far, clinical radionuclide therapy relies on the use of β^- emitter (*e.g.* ^{131}I, ^{90}Y) radiopharmaceuticals which are mainly applied for bone pain palliation and for treatment of neuroendocrine or hematological tumors.[2] However, β^- emitters are not the best suited radionuclides to eliminate disseminated cells or small metastases, since most of the energy of β^- particles is absorbed by the surroundings and not by the target neoplastic cells which accumulate the radiopharmaceutical. For such type of application, α- and Auger electron emitters can be considered a more adequate choice than traditional β^- emitters, but the studies with these radionuclides remain mostly pre-clinical. Nevertheless, Auger radiation therapy appears to be a new possible therapeutic pathway with *in vitro* experimental results already demonstrated for ^{125}I, ^{111}In and ^{99m}Tc.[3–8]

^{99m}Tc, the most used γ-emitter in SPECT (single photon emission computed tomography) imaging, emits also 4 Auger electrons per decay. These low energy electrons provide a high linear energy transfer (high LET) in association with a short tissue penetration, being therefore optimal for treatment of individual cancer cells. However, such application requires a selective accumulation of the radionuclide into individual tumor cells, namely in the nucleus, being highly toxic only when the Auger emitter is tightly bound to DNA.[1] To ensure the close proximity of the emitting radionuclide to the DNA double helix and a prolonged retention time in the cell it is imperative to design multifunctional compounds bearing a DNA-binding unit.[3,9] For ^{99m}Tc, Alberto *et al.* pioneered the study of such type of compounds and demonstrated *in vitro* that the Auger electrons emitted by ^{99m}Tc strongly affect the structure of plasmid DNA with induction of double strand breaks.[8] In our research group, we have also studied and evaluated Re(I)/^{99m}Tc(I) tricarbonyl complexes anchored by pyrazolyl-diamine chelators and bearing anthracenyl groups for DNA binding.[10–12] Our findings were encouraging since some of the anthracenyl-containing ^{99m}Tc(I) tricarbonyl complexes rapidly entered the cells, accumulated inside the nucleus and exhibited a strong radiotoxic effect in murine melanoma cells with an apoptotic cellular outcome. However, the evaluated complexes only presented a moderate affinity to DNA and did not behave as perfect intercalators. Moreover, the anthracene chromophore did not display the best emission properties to allow the follow-up of the cellular trafficking of the Re congeners by fluorescence microscopy. To get a deeper insight into the relevance of pyrazolyl-diamine ^{99m}Tc(I) tricarbonyl complexes in the design of

[a]*Unidade de Ciências Químicas e Radiofarmacêuticas, ITN, Estrada Nacional 10, 2686-953 Sacavém, Portugal. E-mail: isantos@itn.pt*
[b]*Centro de Química Estrutural, IST, TU Lisbon, Av. Rovisco Pais, 1049-001 Lisboa, Portugal*
[c]*IMM, Faculdade de Medicina da Universidade de Lisboa, Av. Prof. Egas Moniz, 1649-028 Lisboa, Portugal*
[d]*Department of Pharmaceutical Sciences, University of Padova, via Marzolo 5, 35131 Padova, Italy*
† Electronic supplementary information (ESI) available: Fig. S1–S9. See DOI: 10.1039/c0ob00073f
‡ Current address: In Vivo Cellular and Molecular Imaging Laboratory, Vrije Universiteit Brussel, Brussels, Belgium
§[2] Current address: Department of Pediatrics, Oncohematology Laboratory, University of Padova *via* Giustiniani 2 35128 Padova, Italy

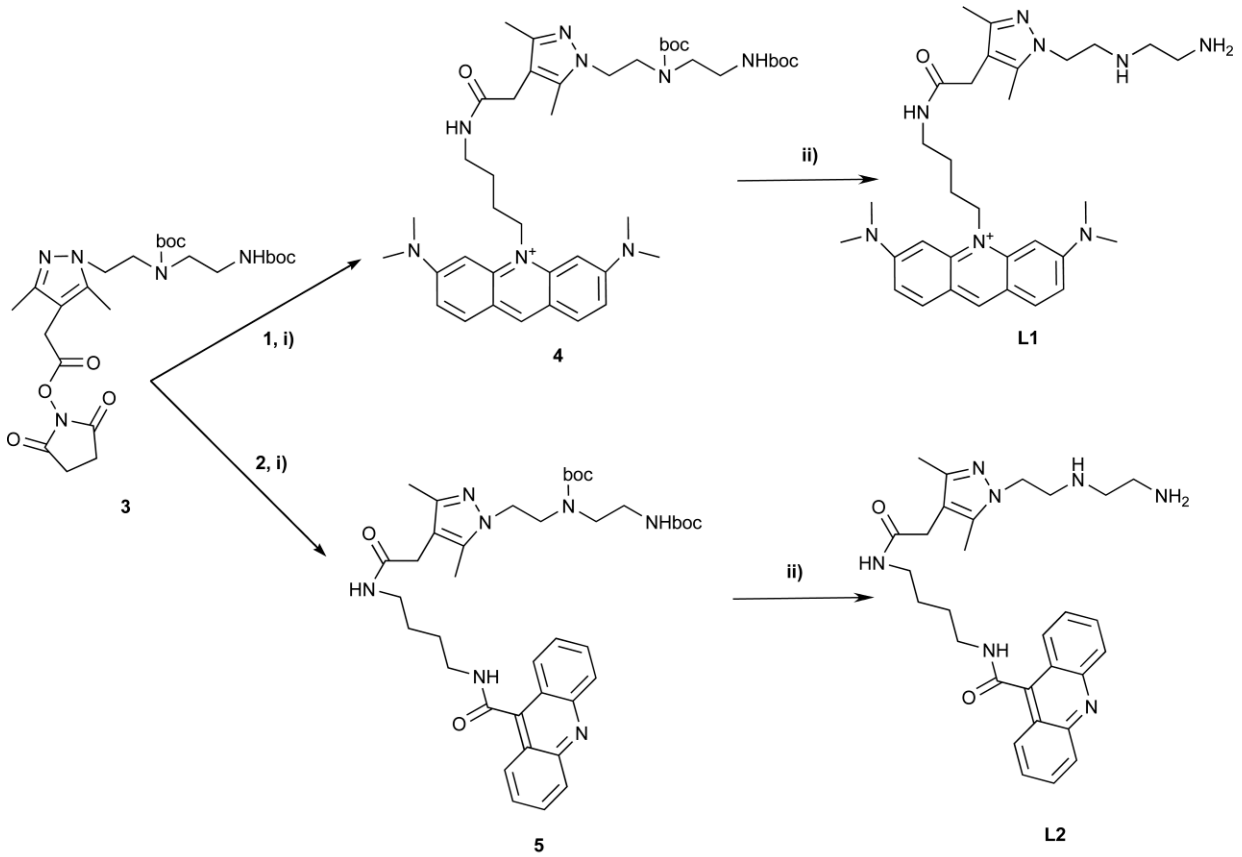

Scheme 1 Synthesis of chelators **L1** and **L2**.

site-directed radiopharmaceuticals for Auger therapy we decided to explore their functionalization with acridine derivatives which are another family of known DNA-binding molecules. By exploring acridine derivatives, we intended to obtain organometallic complexes with a higher DNA-binding affinity and with a better ability to intercalate into the double helix compared with the complexes bearing anthracenyl groups previously evaluated.[10–12] In addition, acridine derivatives are polyaromatic fluorescent planar molecules considered as standard compounds for nuclear staining due to their strong emission properties. Therefore, the use of such chromophores should also allow an easier visualization of the cellular trafficking of the compounds by confocal fluorescence microscopy.

Herein, we report on the synthesis and characterization of new multifunctional pyrazolyl-diamine ligands bearing DNA-binding motifs of the acridine type, which have been attached at the 4-position of the azolyl ring using appropriate methylenic linkers. The synthesis, characterization and *in vitro* evaluation of the respective Re(I)/^{99m}Tc(I) tricarbonyl complexes will be also presented. This includes the study of the interaction with CT-DNA by a variety of spectroscopic techniques, fluorescence microscopy studies, intracellular distribution studies and evaluation of damage in plasmid DNA.

Results and discussion

Synthesis of pyrazolyl containing chelators bearing acridine derivatives and respective metal complexes

Two pyrazolyl diamine chelators bearing acridine derivatives at the 4-position of the pyrazolyl ring (**L1** and **L2**) were synthesized as depicted in Scheme 1. A first step consisted of the synthesis of 10-(4-amino-butyl)-3,6-bis-dimethylamino-acridinium (**1**) and *N*-(4-aminobuthyl)acridine-9-carboxamide (**2**), prepared respectively, from the commercially available acridine orange and 9-acridine carboxylic acid and following described methodologies.[13] Then, chromophores **1** and **2** were conjugated to the protected and activated pyrazolyl-diamine derivative **3**, recently synthesized and characterized in our group.[14] Such conjugation was successfully done in dry DMF, in the presence of DIPEA, at room temperature and after five days of reaction. After appropriate work-up, compounds **4** and **5** were obtained as a dark orange and yellow oil, respectively. The Boc protecting group was then removed by overnight reaction of **4** and **5** with TFA in CH_2Cl_2, at room temperature. The unprotected conjugates were dried under reduced pressure and the crude purified by washing with ethyl acetate (**L1**) or with CH_2Cl_2 followed by column chromatography purification (**L2**). Compounds **L1** and **L2** were then obtained as

a red-orange solid (83% yield) or as a yellow oil (84% yield), respectively.

The new compounds **L1–L2** were characterized by multinuclear NMR spectroscopy (^{1}H, ^{13}C and ^{18}F), ESI-MS, elemental analysis and HPLC. In the ^{1}H NMR spectra of **L1** and **L2** the resonances due to the acridine units were easily identified between 6.5–8.6 ppm for **L1** and 7.5–8.1 ppm for **L2**, while the methylenic protons of the diamine framework appear between 3 and 4.3 ppm for **L1** and between 2.6 and 4.0 ppm for **L2**. For both compounds, two resonances, integrating for three protons each, appear for the 3,5-Me_2 groups of the pyrazolyl ring (at approx. 2 ppm), while the methylenic protons at the 4-position of the same ring appear at about 3.2 ppm. The butylenic protons of the linker between the pyrazolyl diamine framework and the acridine units appear at 1.82 (2H), 1.98 (2H), 3.23 (2H, overlapping with Me groups of the chromophore), and 4.70 (2H) ppm for **L1** and at 1.70 (4H), 2.16 (2H) and 3.61 (2H) ppm for **L2**. In the ^{13}C NMR spectra all the expected resonances could be identified, including the ones due to the TFA. By HPLC one single peak was found for each compound, with retention times of 14.99 min and 10.95 min for **L1** and **L2**, respectively. In the positive mode, the ESI-MS spectra showed prominent peaks at m/z values corresponding to the expected molecular ions: $[M]^+ = 559.1$ for **L1** and $[M + H]^+ = 516.1$ for **L2**.

Reactions of *fac*-$[Re(H_2O)_3(CO)_3]Br$ with **L1** and **L2** in refluxing methanol, followed by column chromatography purification, led to the cationic tricarbonyl complexes **Re1** and **Re2** (Scheme 2).

Complexes **Re1** and **Re2** are red-orange and yellow solids, respectively. They are stable towards air oxidation or hydrolysis and are soluble in water and MeOH. Their characterization was based on IR and multinuclear NMR spectroscopy, ESI-MS, elemental analysis and HPLC. The IR spectra showed intense absorption bands in the range 1890–2024 cm^{-1}, easily assigned to the ν (C≡O) stretching modes of the *fac*-$[Re(CO)_3]^+$ unit. These frequencies compare well with the values found for other Re(I) tricarbonyl complexes anchored by pyrazolyl-diamine chelators of the same family.[15] The ^{1}H NMR data obtained for **Re1** and **Re2** indicate that **L1** and **L2** coordinate to the metal through the pyrazolyl-diamine framework, in a tridentate coordination mode. Such assignment was based mainly on the chemical shift and splitting of the two -NH_2 protons which become diastereotopic after coordination to the metal (3.86 ppm and 5.41 ppm for **Re1**; 3.90 ppm and 5.39 ppm for **Re2**) and methylenic protons of the pyrazolyl-diamine unit which also become diastereotopic originating eight resonances, integrating for one proton each, in the range 2.40 ppm and 4.60 ppm. The pattern obtained is comparable to the one found for other complexes stabilized with chelators of the same family. In **Re1** and **Re2** the resonances from the pyrazolyl-diamine framework exhibit chemical shifts significantly different from those of the corresponding protons in the respective free ligands. In contrast, the signals due to the protons of the chromophoric units, as well as those due to the methylenic and butylenic linkers between the chromophores and the pyrazolyl-diamine backbone, present a splitting and chemical shifts very similar to those of the free ligands, confirming that the chromophore units don't interact with the metal center. In the positive mode, prominent peaks with the expected isotopic pattern could be found in the ESI-MS spectra of **Re1** and **Re2** at m/z 414.9 ($[M]^{2+}$) and 786.0 ($[M]^+$), respectively. The synthesis of the ^{99m}Tc complexes (**Tc1** and **Tc2**) was done in aqueous solution by reaction of *fac*-$[^{99m}Tc(H_2O)_3(CO)_3]^+$ with the appropriate ligand (**L1** or **L2**) at 100 °C for 30 to 40 min and pH 7.4 (Scheme 2). These complexes were obtained in almost quantitative yield (> 98%) using a relatively low final concentration of ligand (10^{-4} M). The chemical identity of **Tc1** and **Tc2** was ascertained by comparison of their HPLC profiles with those of the corresponding rhenium complexes (**Re1–Re2**). The respective retention times are presented in Table 1. These radiocomplexes are stable under physiological conditions, including in the cell culture media (data not shown).

Table 1 Labelling conditions, HPLC retention time and log $P_{o/w}$ values for **Tc1** and **Tc2**

Complex	t/min	T/°C	t_R/min[a]	log $P_{o/w}$ ± SD
Tc1	40	100	17.92 (17.69)	0.56 ± 0.02
Tc2	30	100	16.17 (15.06)	0.74 ± 0.01

[a] The retention time for the Re complexes are in parenthesis

The lipophilicity of complexes **Tc1** and **Tc2** was assessed by measurement of the respective log $P_{o/w}$ values (n-octanol/0.1 M PBS, pH 7.4) using the multiple back extraction method.[16] The complexes **Tc1** and **Tc2** exhibited a hydrophobic character with log $P_{o/w}$ values of 0.56 ± 0.02 and 0.74 ± 0.01, respectively (Table 1).

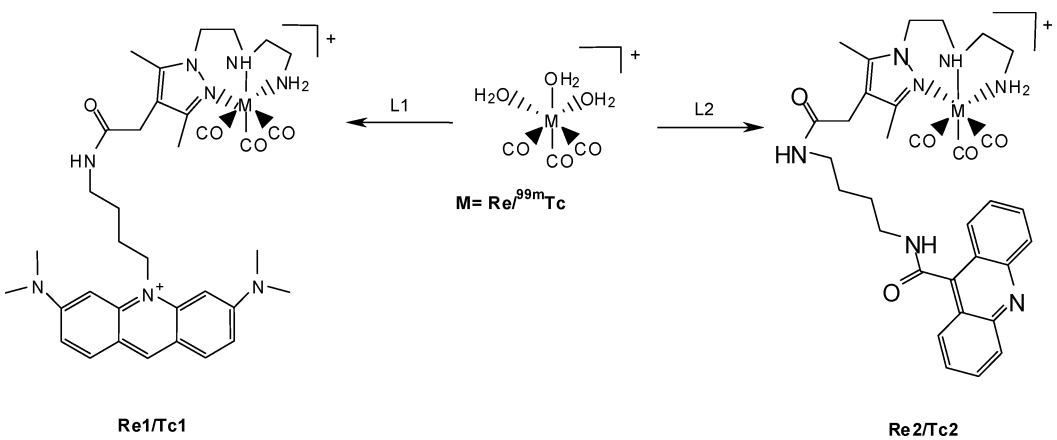

Scheme 2 Synthesis of the Re and ^{99m}Tc complexes.

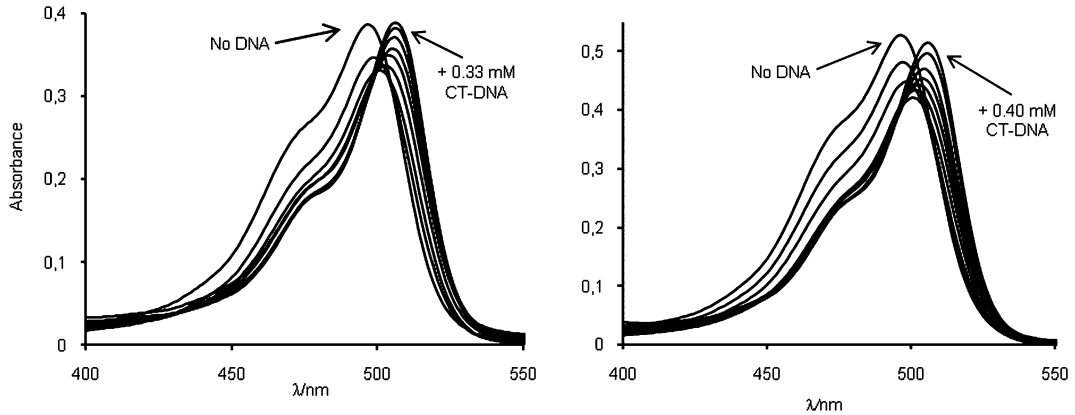

Fig. 1 Absorption spectra of **L1** (4.25×10^{-5} M) and **Re1** (1.5×10^{-5} M) in the presence of increasing amounts of CT-DNA (0.02, 0.04, 0.06, 0.08, 0.13, 0.17, 0.23 and 0.33 mM for **L1**; 0.01, 0.02, 0.04, 0.05, 0.07, 0.10, 0.14, 0.21 and 0.40 mM for **Re1**) in Tris-HCl 0.1M buffer.

DNA-binding studies

The interaction of **L1, L2, Re1** and **Re2** with CT-DNA was evaluated by UV-visible, fluorescence, CD and LD spectroscopies. These studies consisted of monitoring the changes of the bands due to the acridine chromophores upon addition of increasing amounts of DNA.

UV-visible spectroscopy

From the UV-visible titration of compounds **L1** and **Re1** (Fig. 1) it was observed that the absorption peak of the free compounds present a maximum at 496 nm, which is red shifted upon binding of DNA (maximum at 506 nm). Additionally, the shoulder observed at 470 nm changed to 480 nm after interaction of the species with the DNA double helix. This red shift ($\Delta\lambda = 10$ nm) is in agreement with the results reported by other authors for acridine orange (AO) and for a Pt(II) complex bearing a pendant AO fragment, and is consistent with an intercalative binding of the compounds.[17–19] As the DNA concentration increases, the shoulder at 470 nm diminishes in intensity. Such a shoulder can be assigned to the presence of dimeric species, resulting from the self-association of AO rings, their formation being less probable when the compounds bind to DNA. The shape and intensity of the band at 506 nm due to the bound compounds remained fairly constant, indicating that **L1** and **Re1** act most probably as intercalated monomers without any interaction between themselves.

The UV-vis spectra of **L2** and **Re2** (see Fig. S1 in Supplementary Information) show an absorption maximum at 359 nm. Upon addition of CT-DNA, there is a moderate hypochromicity but no bathochromic shift is observed. These findings indicate that these compounds have a low propensity to interact with DNA by intercalation.

Fluorescence spectroscopy

The addition of DNA to solutions of **L1** and **Re1** led to the increase of the emission intensity until a saturation value was reached (Fig. 2). Such enhancement of fluorescence clearly indicates the intercalation of the AO moiety of compounds **L1** and **Re1** into the DNA double helix, as claimed by other authors for different AO derivatives.[13,17]

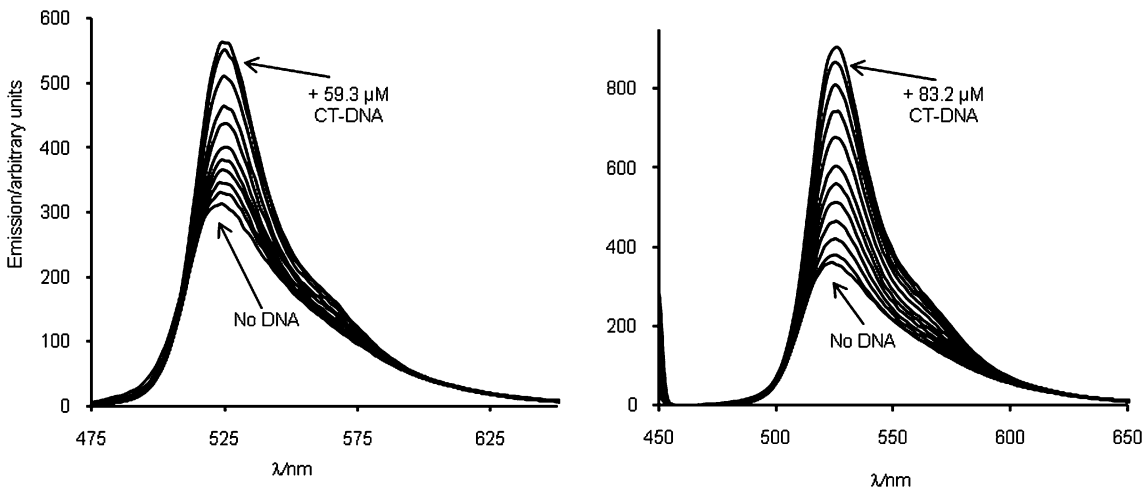

Fig. 2 Fluorescence spectra of **L1** (1.06×10^{-5} M, left) and **Re1** (1.5×10^{-6} M, right) in the presence of increasing amounts of CT-DNA (5.6, 8.4, 11.1, 13.9, 16.6, 21.5, 26.4, 36.0, 50.1 and 59.3 μM for **L1**; 4.0, 7.8, 11.7, 15.5, 19.3, 23.1, 30.1, 37.0, 50.6, 70.4 and 83.2 μM for **Re1**) in Tris-HCL 0.1M buffer. Excitation at 470 nm.

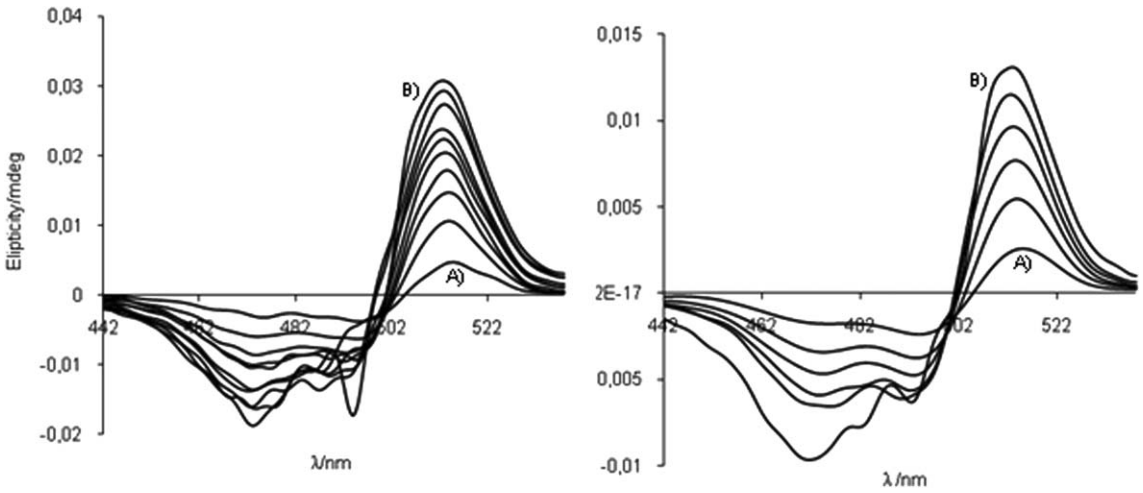

Fig. 3 ICD spectra of compounds **L1** (left) and **Re1** (right) at several ratios of [DNA]/[probe] concentrations for a CT-DNA concentration of 2.5×10^{-5} M $nucl^{-1}$: A) 0.2 eq. of probe; B) 2 eq. of probe.

For **L2** and **Re2**, the addition of DNA induces a quenching of the fluorescence (Fig. S2, S. I.), as commonly found for acridine derivatives due to an energetically favorable electron-transfer reaction from the DNA bases to the acridine moiety.[20] However, only a slight fluorescence quenching was observed, particularly in the case of **Re2**. This certainly reflects the low affinity of these compounds to DNA, as already indicated by the UV-vis experiments.

Induced circular (CD) and linear dichroism (LD)

The compounds **L1, Re1** and **L2, Re2** do not present CD spectra, in agreement with the expected non-chirality of the molecules. However, their association with the right-handed DNA helix should led to ICD spectra in the range where the acridine or AO chromophores absorb (400–525 nm). From the compounds studied, only **L1** and **Re1** show positive ICD spectra in the expected spectral range (Fig. 3), as a result of the close proximity between the chromophores and the biomolecule. For 0.2 equivalents of DNA we have observed one positive band at 516 nm and two negative bands at 475 nm and 489 nm with intensities varying greatly with increasing amounts of the chromophores. These bands can be assigned to intercalated compounds by comparison with the ICD spectra reported previously for AO bound to DNA.[17]

For compounds **L2** and **Re2** it was not possible to register any changes in the CD spectra of the species in the presence of CT-DNA, showing once again the poor interaction ability of these compounds with the biomolecule.

LD studies were performed in order to get better information about the spatial orientation of the chromophore relative to the DNA double helix. Both **L1** and **Re1** induced a strong increase in the signal intensity for the DNA band (230–300 nm) indicating that the DNA becomes more oriented within the hydrodynamic field upon interaction because of stiffening of the helix on intercalation of these compounds (Fig. 4). Furthermore, a negative signal also emerged in the chromophore region (400–525 nm) which suggests an intercalation binding mode for **L1** and **Re1**. The nearly constant value of LD_r in this spectral range confirms the perfect intercalation for both species.

Table 2 Intrinsic binding constants (K) for **L1** and **Re1**

		$K/M^{-1} \times 10^5$	
Spectroscopic technique	Model	**L1**	**Re1**
UV-Visible	Scatchard	1.71 ± 0.01	2.50 ± 0.01
	Kaminoh	1.75 ± 0.15	2.33 ± 0.39
Fluorescence	Scatchard	1.53 ± 0.01	2.26 ± 0.01
	Kaminoh	1.93 ± 0.22	2.36 ± 0.02
	McGhee von Hippel	1.93 ± 0.86	1.17 ± 0.68
		$n = 2.7$	$n = 17.8$

For compounds **L2** and **Re2**, the addition of DNA also led to the appearance of a negative band in the chromophore absorption region (300–400 nm) (Fig. S3, S.I.). However, even for the highest concentrations of DNA, its intensity was much lower than the intensity of the bands induced by **L1** and **Re1**. Therefore, the LD studies confirmed once again that compounds **L2** and **Re2** have a lower affinity towards the DNA double helix in comparison with **L1** and **Re1**. The presence of these negative bands suggests that **L2** and **Re2** can intercalate into the DNA double helix. However, the LD_r signal in this spectral range is largely wavelength dependent and its intensity is higher than that of DNA alone, indicating that these compounds are only partially intercalated.

DNA binding constant

The data obtained for compounds **L1** and **Re1** in the UV-visible and fluorescence titrations were used to obtain the intrinsic binding constants (K) (Table 2) by adjustment to different mathematical and computational models (see Experimental Section). Simple Scatchard and Kaminoh models were fitted to the UV-vis and fluorescence data; the fluorescence data were also fitted to the non-cooperative McGhee von Hippel model. As discussed above, compounds **L2** and **Re2** revealed a poor interaction with the DNA and no model could be adjusted to determine the respective binding constants.

For **L1**, the adjustment of the McGhee von Hippel model gave a K value of $(1.93 \pm 0.86) \times 10^5$ M and a binding size site (n) of

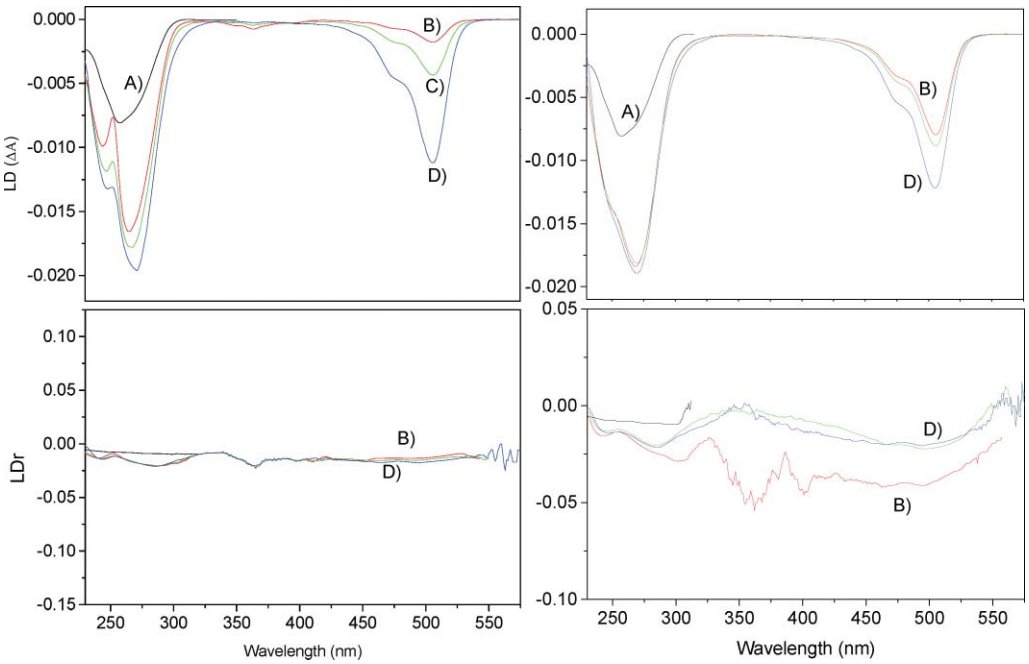

Fig. 4 Linear dichroism (LD, upper panels) and reduced linear dichroism (LDr, lower panels) of **L1** (left) and **Re1** (right) at different [DNA]/[probe] molar ratios: A) no probe; B) 25; C) 12; D) 5. Spectra were recorded in 10 mM phosphate buffer at pH 7.2.

2.7. These values are comparable with those reported for acridine orange, particularly in which concerns the *n* value that is consistent with an intercalative binding of the molecule.[21–23] By contrast, a large *n* value (17.8) was determined for **Re1** which indicates that the obtained data are not consistent with a nearest neighbor exclusion intercalation model. This might result from the involvement of different binding modes in the range of concentrations needed to reach saturation in the case of **Re1**.[24] In fact, **L1** reached saturation at 59.3 μM of CT-DNA whereas **Re1** required 83.2 μM of CT-DNA to reach saturation. Complex **Re1** has a larger net positive charge (+2) that may favor electrostatic interactions with the phosphate groups from the outer-part of the DNA double helix, justifying the highest DNA concentration needed to reach saturation.

As discussed above, the McGhee von Hippel model was not properly fitted to fluorescent data obtained for the DNA titration of **Re1**. Therefore, the binding constant calculated based on such adjustment should be considered with caution. In order to compare the DNA affinity of **L1** and **Re1**, the respective binding constants (*K*) were determined using Scatchard and Kaminoh models, based on the UV-vis and fluorescence data. Based on these models, the *K* values determined for **Re1**, spanning between $(2.26 \pm 0.01) \times 10^5$ and $(2.50 \pm 0.01) \times 10^5$ M^{-1}, were consistently higher than those found for **L1** ($(1.53 \pm 0.01) \times 10^5$–$(1.93 \pm 0.22) \times 10^5$ M^{-1}). This certainly reflects the higher positive charge of **Re1** that may favor electrostatic interactions with the DNA phosphate groups.

Cellular and nuclear uptake studies

When designing a ^{99m}Tc-radiopharmaceutical, namely as a potential candidate for Auger electron therapy, it is very important to quantify the cellular and nuclear uptake of the compounds but is also important to follow the trafficking of the compounds at cellular and subcellular level, in real time. The cell uptake quantification can be easily done using the radioactive ^{99m}Tc-complexes, but the trafficking can only be evaluated using analogous and fluorescent Re complexes.

Taking advantage of the fluorescence emission characteristics of the chromophore units of the newly synthesized compounds, the cellular uptake for the ligands **L1** and **L2** and the corresponding complexes, **Re1** and **Re2**, was assessed by fluorescence microscopy in B16F1 murine melanoma cells. Compounds **L1** and **Re1** were detected by the emission of green fluorescence and the nuclear localization was evaluated by comparison with the nuclear stain DAPI. Compounds **L2** and **Re2** were detected by the emission of blue fluorescence and the nuclear localization was evaluated by comparison with the nuclear stain DRAQ5.

L1 and **Re1** were detected in the cytoplasm and in the nucleus, specifically in the nucleoli (data not shown). **L2** and **Re2** also localize in the cytoplasm and in the nucleus of the cells but present a less intense emission of fluorescence. This lower emission intensity led to a lower definition of the images, due to the longer exposure time required for the capture (data not shown). Due to the promising results obtained for **L1** and **Re1** the cellular uptake of these compounds was further evaluated by confocal laser-scanning fluorescence microscopy, which confirmed the cellular localization of **L1** and **Re1** in the cytoplasm and nucleus in association with the nucleoli (Fig. 5).

To quantify the cellular and nuclear internalization found for **Re1** using fluorescence microscopy, we have studied the behavior of **Tc1** with the same cell line. These studies were performed using B16F1 murine melanoma cells and the HPLC purified **Tc1** complex.

The cellular internalization of **Tc1** was performed at 37 °C and was time-dependent (Fig. 6). Moderate levels of internalization

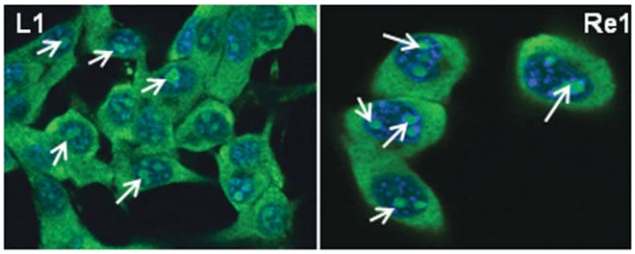

Fig. 5 Uptake of compounds **L1** and **Re1** (70 μM) by B16F1 murine melanoma cells evaluated by confocal fluorescence microscopy (blue: nuclei; white arrows: nucleoli).

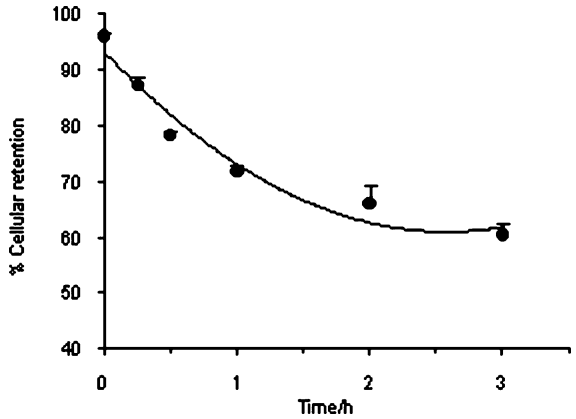

Fig. 7 Cellular retention of the internalized complex **Tc1** in B16F1 cells over time at 37 °C (mean ± standard deviation, $n = 3$).

were reached. For example, at 5 h post-incubation a value of 7.8% was obtained, when internalization is expressed as a percentage of total activity (Fig. 6A). For the same time of incubation, approximately 34% of the bound activity (activity on the membrane and inside the cell) was taken up and internalized by the cells (Fig. 6B).

The cellular retention of **Tc1** was evaluated at different time points, after 3 h of internalization (Fig. 7). The radiocomplex was slowly released from the cells into the culture medium, with about 60% of the initially internalized complex still remaining inside the cells at 3 h post-incubation.

Nuclear internalization of compound **Tc1** in B16F1 cells was also determined. The percentage of activity internalized into the nucleus per total activity is presented in Fig. 8A. At 6 h post-incubation, 3.8% of the administered compound was internalized into the cell nucleus.

The nuclear internalization was also determined by the ratio between the activities internalized into the nucleus and the cell-bound activity (Fig. 8B). Such calculation gives a more accurate measure of the ability of the complex to pass from the cytoplasm to the nucleus. As can be seen in Fig. 8B, the nuclear internalization is very fast and the percentage of compound inside the nucleus is higher than that outside (*i.e.*, cytoplasm and cell membrane). After 30 min, 67.2% of **Tc1** was found in the nucleus. This shows that the radioactive compound rapidly diffuses to the cell nucleus after being internalized by the cell, reflecting most probably its affinity to DNA.

Plasmid DNA studies

Since **Re1** was shown to interact strongly with CT-DNA and the congener **Tc1** presented an enhanced ability to target the nucleus, we decided to evaluate if the Auger electrons emitted by ^{99m}Tc would induce damage on plasmid DNA, upon formation of single-strand breaks (SSB) or double-strand breaks (DSB). These studies were also performed for the congener **Re1** and for $[^{99m}TcO_4]^-$, in order to check if the eventual damage is due to the radioactive character of **Tc1** combined with its ability to intercalate into the DNA double helix. The non-radioactive **Re1** was evaluated in a 10^{-8} M concentration, corresponding approximately to the molar concentration used for **Tc1**. **Tc1** and $[^{99m}TcO_4]^-$ were studied using the same amount of radioactivity (150–310 μCi). Samples of $[^{99m}TcO_4]^-$ and complexes **Re1** and **Tc1** were incubated with plasmid DNA (puc19) and the formation of strand breaks was analyzed by agarose gel electrophoresis. As can be seen in Fig. 9, **Tc1** (C and D) induced a more pronounced reduction of the supercoiled (sc) band intensity compared with complex **Re1** (G) and with $[^{99m}TcO_4]^-$ (E and F). The total plasmid DNA containing strand breaks corresponded to more than 30% in the case of **Tc1**, roughly to 15% for **Re1** and to less than 6% for $[^{99m}TcO_4]^-$. For all the compounds, the damaged DNA is uniquely in the open

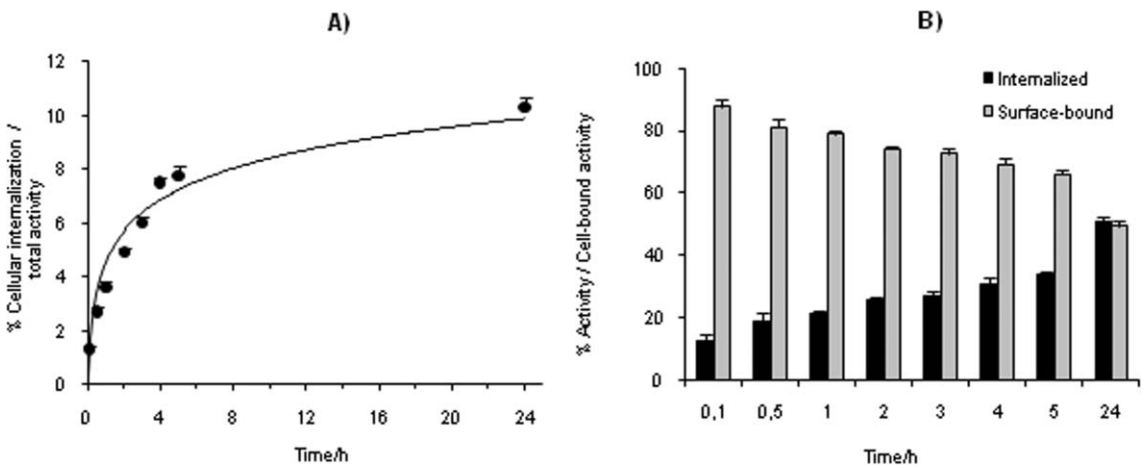

Fig. 6 Cellular internalization of **Tc1** at 37 °C in B16F1 murine melanoma cells. A) Internalization expressed as a percentage of total activity; B) internalized and surface bound activity expressed as a fraction of cell-bound activity (mean ± standard deviation, $n = 3$).

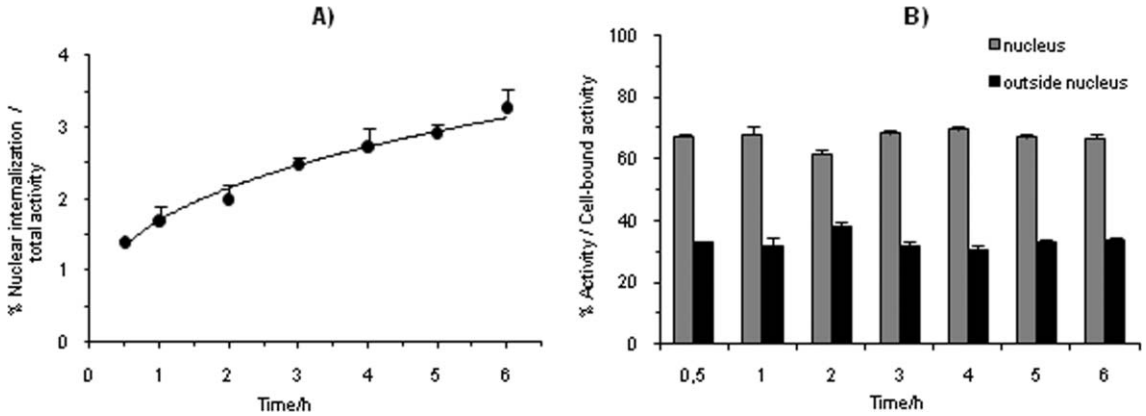

Fig. 8 Nuclear internalization of **Tc1** at 37 °C in B16F1 murine melanoma cells. A) Nuclear internalization expressed by total activity; B) activity inside the nucleus and outside the nucleus expressed as a percentage of cell-bound activity (mean ± standard deviation, $n = 3$).

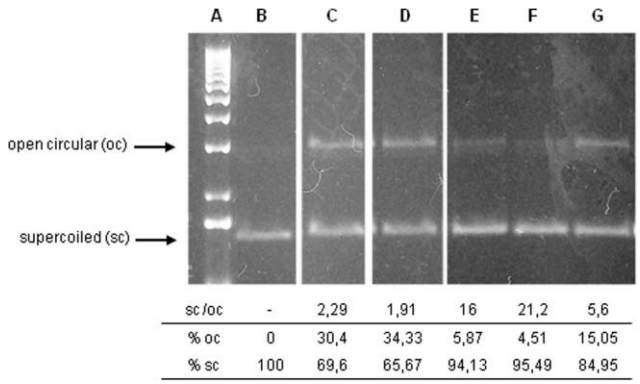

sc/oc	-	2,29	1,91	16	21,2	5,6
% oc	0	30,4	34,33	5,87	4,51	15,05
% sc	100	69,6	65,67	94,13	95,49	84,95

Fig. 9 Cleavage of supercoiled (sc) puc19 DNA, after 48 h of incubation at room temperature in Tris (pH 7.4): **A** – molecular weight marker – 1 Kb DNA ladder; **B** – control (DNA + buffer); **C** – DNA + **Tc1**, 310 μCi; **D** – DNA + **Tc1**, 150 μCi; **E** – DNA + $[^{99m}TcO_4]^-$, 310 μCi; **F** – DNA + $[^{99m}TcO_4]^-$, 150 μCi; **G** – DNA + **Re1** (10^{-8} M).

circular (oc) form, no linear form being detected. In summary, complex **Tc1** induces more easily SSB in plasmid DNA compared with **Re1** and with $[^{99m}TcO_4]^-$. This probably reflects the expected high affinity of **Tc1** to DNA and its ability to act as a perfect intercalator, taking into consideration the interaction studies with DNA performed for the isostructural **Re1**. However, **Tc1** was unable to provoke DSBs as would be expected if the emission of Auger electrons by the ^{99m}Tc radionuclide could occur in a close proximity to DNA. For ^{125}I-labelled molecules, it has been reported in several instances that small changes in the position of the decay site may have strong effects on the yields of SSBs and DSBs.[4] Eventually, the butylenic linker used to attach the AO fragment to the planar azolyl ring allows a perfect intercalation of the chromophore but is too long to assure the proximity of the radiometal to the DNA bases, necessary to have DSBs induced by the emitted Auger electrons.

Concluding remarks

Novel pyrazolyl-diamine chelators bearing acridine derivatives at the 4-position of the pyrazolyl ring have been synthesized and characterized (**L1, L2**) and used to prepare Re and ^{99m}Tc tricarbonyl complexes (**Re1, Tc1, Re2, Tc2**). The interaction of all these compounds with CT-DNA was studied using different spectroscopic techniques. Based on UV-visible and fluorescence spectroscopy, as well as on circular and linear dichroism it was found that **L1** and **Re1** act as DNA intercalators, while **L2** and **Re2** have a much lower affinity towards the DNA double helix. Using different mathematical and computational models the results obtained on UV-visible and fluorescence were used to calculate intrinsic binding constants. For **L2** and **Re2** no model could be adjusted, certainly due to the poor interaction of these compounds with DNA. Using the McGhee von Hippel model, the K and n values obtained for **L1** compare well with the ones reported previously for acridine orange, but the values found for **Re1** must be taken with caution, mainly due to the high value found for the binding size site ($n = 17.8$, **Re1**), which may reflect the larger net positive charge of **Re1** (+2). Based on the fluorescence emission of the AO and on the possibility of preparing analogous Re and Tc tricarbonyl complexes, it was found that **Re1** and ^{99m}**Tc1** internalize significantly and are retained in the nucleus of B16F1 murine melanoma cells. Studies with plasmid DNA also confirm that **Tc1** induces reduction of the sc band intensity, reflecting the expected high affinity of the complex to DNA, its ability to intercalate and the emission of Auger electrons. The absence of DSBs may indicate that a linker shorter than the butylenic one has to be explored in our studies, to assure a closer proximity of the radiometal to the DNA. The results presented herein, together with the stability and versatility of this type of complexes, encourage the synthesis of ^{99m}Tc trifunctional complexes for cell-specific and DNA targeting, as well as the evaluation of their therapeutic effect as Auger-emitters.

Experimental section

Chemistry

All chemicals were of reagent grade. Solvents were dried and distilled prior to use according to described procedures.[25] Unless stated otherwise, the syntheses of the ligands and complexes were carried under a nitrogen atmosphere, using standard Schlenk techniques and dry solvents; the work-up procedures were performed under air. Compounds 2-(4-bromobutyl)isoindoline-1,3-dione,[26] and *tert*-butyl *N*-(2-{[(*tert*-butoxy)carbonyl](2-{4-[2-(2,5-dioxopyrrolidin-1-yl)-2-oxoethyl]-3,5-dimethylpyrazol-1-yl}ethyl)amino}ethyl)carbamate (**3**)[14] were prepared according to

published methods. The starting material *fac*-[$Re(H_2O)_3(CO)_3$]Br was synthesized by the literature method.[27]

Na[$^{99m}TcO_4$] was eluted from a commercial $^{99}Mo/^{99m}Tc$ generator, using 0.9% saline. ^1H and ^{13}C NMR spectra were recorded on a Varian Unity 300 MHz spectrometer; ^1H and ^{13}C chemical shifts are given in ppm and were referenced to the residual solvent resonances relative to $SiMe_4$. The NMR samples were prepared in $CDCl_3$ or CD_3OD. *J* values are given in Hz. IR spectra were recorded in the range 4000–200 cm^{-1} as KBr pellets on a Bruker Tensor 27 spectrometer. Electrospray ionisation mass spectrometry (ESI-MS) was performed using a Bruker HCT electrospray ionization quadrupole ion trap mass spectrometer. Elemental analyses were performed on a Perkin-Elmer automatic analyser.

Thin layer chromatography (TLC) was done on Merck silica gel 60 F254 plates. Column chromatography was performed with silica gel 60 (Merck). HPLC analysis of the ligands, Re complexes and ^{99m}Tc complexes was performed on a Perkin-Elmer LC pump 200 coupled to a LC 290 tunable UV–vis detector and to a Berthold LB-507A radiometric detector, using an analytic Macherey-Nagel C18 reversed-phase column Nucleosil 100-5, 250 × 4 mm, with a flow rate of 0.9 mL min^{-1}; UV detection, 254 nm; eluents, A: aqueous 0.1% CF_3CO_2H solution, B: acetonitrile; method: 0–3 min, 100% A; 3–3.1 min, 100%–75% A; 3.1–9 min, 75% A; 9–9.1 min 75%–66% A; 9.1–18 min, 66%–0% A; 18–25 min, 0% A; 25–25.1 min, 0%–100% A; 25.1–30 min, 100% A. HPLC purification of the radioactive compound was done with a semi-preparative Macherey-Nagel EP 250 × 8 Nucleosil 100-7 C18 reversed-phase column at a flow rate of 2.0 mL min^{-1} using the same methodology as for analytical HPLC. Radioactivity measurements were done using a ionization chamber Aloka, Curiemeter IGC-3 or a γ-counter Berthold, LB 2111.

Synthesis of the bifunctional ligands L1 and L2

10-(4-Amino-butyl)-3,6-bis-dimethylamino-acridinium (1). *p*-Xylol (90 cm^3) was added to acridine orange (1 g, 3.769 mmol) and 2-(4-bromobutyl)isoindoline-1,3-dione (3.2 g, 11.306 mmol) and refluxed overnight. The reaction mixture was filtered and the solid obtained was washed with acetone, dried under reduced pressure and purified by column chromatography (eluent: CH_2Cl_2 (98–80%)/MeOH (2–20%)) giving 3,6-bis(dimethylamino)-10-(4-(1,3-dioxoisoindolin-2-yl)butyl)acridinium (0.597 g, 31%) as a red–orange solid. δ_H(300 MHz; $CDCl_3$; Me_4Si) 1.90 (2H, m, CH_2), 2.06 (2H, t, *J* 6.6, CH_2), 3.25 (12H, s, $4CH_3$), 3.80 (2H, t, *J* 6.6, CH_2), 4.88 (2H, m, CH_2), 6.51 (2H, s, 2CH-Ar), 6.94 (2H, d, *J* 8.7, 2CH-Ar), 7.68 (2H, m, 2CH-Ar), 7.74 (2H, m, 2CH-Ar), 7.81 (2H, d, *J* 8.7, 2CH-Ar), 8.63 (1H, s, CH-Ar). Hydrazine hydrate (0.471 g, 9.416 mmol) was added to a suspension of 3,6-bis(dimethylamino)-10-(4-(1,3-dioxoisoindolin-2-yl)butyl)acridinium in a mixture of methanol and ethanol (3 : 1) and refluxed overnight. After addition of 4 cm^3 of concentrated HCl (37%) a white solid of phthalic acid hydrazide precipitated. After filtration the pH of the solution was adjusted to about 9 with 3 M NaOH. The reaction mixture was extracted with chloroform (3 × 50 cm^3) and the combined organic phases were dried over $MgSO_4$ and evaporated under reduced pressure to give **1** (0.450 g, 95%) as a red–orange solid. δ_H(300 MHz; CD_3OD; Me_4Si) 1.95 (2H, m, CH_2), 2.08 (2H, m, CH_2), 3.01 (2H, t, *J* 6.9, CH_2), 3.33 (12H, s, $4CH_3$), 4.78 (2H, t, *J* 8.1, CH_2), 6.68 (2H, d, *J* 2.1, 2CH-Ar), 7.26 (2H, dd, *J* 2.1, *J* 2.4 and *J* 9.0, 2CH-Ar), 7.90 (2H, d, *J* 9.3, 2CH-Ar), 8.66 (1H, s, CH-Ar); δ_C(75.4 MHz; CD_3OD; Me_4Si) 24.42 (CH_2), 26.40 (CH_2), 40.57 (CH_2), 40.95 ($4CH_3$), 47.69 (CH_2), 93.61 (2CH-Ar), 115.43 (2CH-Ar), 118.38 (2C-Ar), 134.38 (2CH-Ar), 143.95 (2C-Ar), 144.30 (CH-Ar), 157.32 (2C-Ar).

***N*-(4-Aminobutyl)acridine-9-carboxamide (2).** After being stirred for two hours at room temperature, a suspension of 9-acridine carboxylic acid (0.460 g, 2.061 mmol) and benzotriazole-1-yl-oxy-tris-(dimethylamino)-phosphonium hexafluorophosphate (BOP) (1 g, 2.261 mmol) in 25 cm^3 of CH_2Cl_2, was cooled to 0 °C and 1,4-diamino butane (1 cm^3, 10.275 mmol) was added drop by drop. The reaction mixture was stirred again for 2 days at room temperature. The solvent was removed and the residue was purified by column chromatography (eluent: $CHCl_3$ (95–0%)/MeOH (5-80%)/NH_4OH 25% (0–20%)) to give **5** (0.415 g, 69%) as a yellow solid. δ_H(300 MHz; CD_3OD; Me_4Si) 1.79 (4H, m, $2CH_2$), 2.85 (2H, t, *J* 6.9, CH_2), 3.65 (2H, t, *J* 6.3, CH_2), 7.67 (2H, m, 2CH-Ar), 7.87 (2H, m, 2CH-Ar), 8.06 (2H, d, *J* 8.7, 2CH-Ar), 8.19 (2H, d, *J* 9.0, 2CH-Ar); δ_C(75.4 MHz; CD_3OD; Me_4Si) 27.72 (CH_2), 29.51 (CH_2), 40.76 (CH_2), 41.51 (CH_2), 123.65 (2C-Ar), 126.56 (2CH-Ar), 128.21 (2CH-Ar), 129.56 (2CH-Ar), 132.05 (2CH-Ar), 132.33 (C-Ar), 149.57 (2C-Ar), 169.21 (C=O).

10-(4-(2-(1-(2-*tert*-Butoxycarbonyl(2-(*tert*-butoxycarbonyl-amino)ethyl)amino)ethyl)-3,5-dimethylpyrazol-4-yl)acetamido)-butyl)-3,6-bis(dimethylamino)acridinium (4). To a solution of **1** (0.045 g, 0,107 mmol) in dry DMF (20 cm^3) kept stirring for one hour at room temperature, was added a solution of **3** (0.055 g, 0.102 mmol) and DIPEA (19 µl, 0.107 mmol) in DMF (15 cm^3). After five days the solvent was removed under reduced pressure and the dry residue obtained was purified by column chromatography (eluent: $CHCl_3$ (95–60%)/MeOH (5–35%)/NH_4OH 25% (0–5%)) to give **4** (0.054 g, 63%) as a dark orange solid. δ_H(300 MHz; $CDCl_3$; Me_4Si) 1.35 (18H, m, $6CH_3$ (BOC)), 1.95 (4H, m, $2CH_2$), 2.07 (6H, m, $2CH_3$), 3.05 (4H, m, $2CH_2$), 3.31 (18H, m, $3CH_2$, $4CH_3$), 3.99 (2H, m, CH_2), 4.70 (2H, m, CH_2), 5.27 (1H, s br, NH), 5.73 (1H, s, br, NH), 6.57 (2H, s, 2CH-Ar), 6.97 (2H, d, *J* 9.0, 2CH-Ar), 7.75 (2H, t, *J* 8.7 and *J* 9.0, 2CH-Ar), 8.47 (1H, d, *J* 15.9, CH-Ar); δ_C(75.4 MHz; $CDCl_3$; Me_4Si) 9.14 (CH_3), 11.37 (CH_3), 17.95 (CH_2), 25.03 (CH_2), 27.77 ($3CH_3$, BOC), 30.74 (CH_2), 38.91 (CH_2), 40.46 ($4CH_3$), 41.68 (CH_2), 47.45 (CH_2), 53.23 ($2CH_2$), 57.13 (CH_2), 78.42 (C-BOC), 79.31 (C-BOC), 92.13 (2CH-Ar), 109.89 ($C_{4\text{-pz}}$), 113.55 (2CH-Ar), 116.52 (2C-Ar), 132.86 (2CH-Ar), 137.48 ($C_{3/5\text{-pz}}$), 142.05 (2C-Ar), 146.11 ($C_{3/5\text{-pz}}$), 155.08 (2CH-Ar), 155.60 (2C=O, BOC), 171.29 (C=O).

10-(4-(2-(1-(2-(2-Aminoethylamino)ethyl)-3,5-dimethyl-1*H*-pyrazol-4-ylacetamido)butyl)-3,6-bis(dimethylamino))acridinium (L1). **4** (0.244 g, 0.290 mmol) was dissolved in a mixture of TFA (2 cm^3, 25.960 mmol) and CH_2Cl_2 (1 : 1) and stirred at room temperature overnight. After that period of time the solvent was removed under reduced pressure and the solid was washed with ethyl acetate to give **L1(CF_3CO_2)·3.5TFA** (0.258 g, 0.241 mmol, 83%) as a red–orange solid (Found: C, 45.29; H, 5.27; N, 11.04. $C_{34}H_{47}F_3N_8O_2 \cdot 3.5(CF_3CO_2H)$ requires C, 45.94; H, 4.76; N, 10.46%); δ_H(300 MHz; CD_3OD; Me_4Si) 1.82 (2H, m, CH_2), 1.98 (2H, m, CH_2), 2.03 (3H, s, CH_3), 2.15 (3H, s, CH_3),

3.23 (20H, m, $4CH_2$, $4CH_3$), 3.50 (2H, t, *J* 5.7, CH_2), 4.31 (2H, t, *J* 5.7, CH_2), 4.70 (2H, t, *J* 7.8, CH_2), 6.64 (2H, s, 2CH-Ar), 7.24 (2H, dd, *J* 1.5, *J* 2.1 and *J* 9.0, 2CH-Ar), 7.87 (2H, d, *J* 9.0, 2CH-Ar), 8.62 (1H, s, CH-Ar); δ_C(75.4 MHz; CD_3OD; Me_4Si) 9.37 (CH_3), 11.88 (CH_3), 24.79 (CH_2), 28.27 (CH_2), 31.30 (CH_2), 36.85 (CH_2), 40.21 (CH_2), 40.84 ($4CH_3$), 45.06 (CH_2), 45.80 (CH_2), 93.62 (2CH-Ar), 112.04 ($C_{4\text{-pz}}$), 115.51 (2CH-Ar), 118.12 (C_{TFA}) 118.47 (2C-Ar), 134.37 (2CH-Ar), 140.32 ($C_{3/5\text{-pz}}$), 144.02 (2C-Ar), 144.29 (1CH-Ar), 149.15 ($C_{3/5\text{-pz}}$), 157.35 (2CH-Ar), 163.56 (C_{TFA}), 173.83 (C=O); δ_F(281.98 MHz; CD_3OD; Me_4Si) -76.39 (CF_3CO_2H); t_R = 14.99 min (100-5 C18, 0.9 mL min^{-1}); *m*/*z* (ESI-MS) 559.1 $[M]^+$, 280.0 $[M + H]^{2+}$.

***N*-(4-(2-(1-(2-(*tert*-Butoxycarbonyl)-2-(*tert*-butoxycarbonylamino)ethyl)amino)ethyl)-3,5-dimethyl-1*H*-pyrazol-4-ylacetamido)butyl)acridine-9-carboxamide (5).** A solution of **3** (0.516 mmol) and DIPEA (0.151 g, 0.516 mmol) in dry DMF (10 cm^3) was added to a solution of **2** (0.264 g, 0.491 mmol) in DMF (30 cm^3) and stirred for 5 days at room temperature. The solvent was then removed and the residue was purified by column chromatography (eluent: $CHCl_3$ (90–54%)/MeOH (10–46%)) to give **5** (0.294 g, 84%) as a yellow oil. δ_H(300 MHz; $CDCl_3$; Me_4Si) 1.25 (9H, s, $3CH_3$ (BOC)), 1.37 (9H, s, $3CH_3$ (BOC)), 1.58 (2H, m, CH_2), 1.68 (2H, m, CH_2), 1.98 (3H, s, CH_3), 2.00 (3H, s, CH_3), 3.08 (2H, s, CH_2), 3.14 (8H, m, $4CH_2$), 3.38 (1H, NH), 3.55 (2H, m, CH_2), 3.89 (2H, s, CH_2), 6.59 (1H, s br, NH, amide), 6.67 (1H, s br, NH, amide), 7.37 (2H, t, *J* 8.1 and *J* 6.6, 2CH-Ar), 7.59 (2H, t, *J* 8.4 and *J* 6.9, 2CH-Ar), 7.82 (2H, d, *J* 8.4, 2CH-Ar), 7.94 (2H, d, *J* 9.0, 2CH-Ar); δ_C(75.4 MHz; $CDCl_3$; Me_4Si) 9.07 (CH_3), 11.17 (CH_3), 26.49 (CH_2), 26.71 (CH_2), 27.77 ($6CH_3$ (BOC)), 28.14 ($6CH_3$ (BOC)), 30.80 (CH_2), 36.01 (CH_2), 38.43 (CH_2), 38.89 (CH_2), 39.34 (CH_2), 47.17 (CH_2), 48.62 (CH_2), 78.55 (C-BOC), 79.21 (C-BOC), 109.43 ($C_{4\text{-pz}}$), 121.62 (2C-Ar), 124.97 (2CH-Ar), 126.10 (2CH-Ar), 128.68 (2CH-Ar), 129.91 (2CH-Ar), 137.38 (C-Ar), 141.30 ($C_{3/5\text{-pz}}$), 145.77 (2C-Ar), 147.70 ($C_{3/5\text{-pz}}$), 155.05 (C=O, BOC), 155.77 (C=O, BOC), 166.59 (C=O), 170.75 (C=O).

***N*-(4-(2-(1-(2-(2-Aminoethylamino)ethyl)-3,5-dimethyl-1*H*-pyrazol-4-yl)acetamido)butyl)acridine-9-carboxamide (L2). 5** (0.294 g, 0.411 mmol) was dissolved in a mixture of TFA (2 cm^3, 25.960 mmol) and CH_2Cl_2 (1 : 1) and stirred overnight at room temperature. After that time the solvent was removed under reduced pressure, the residue was washed with $CHCl_3$ and purified by column chromatography (eluent: $CHCl_3$ (95–70%)/MeOH (5–20%)/NH_4OH 25% (0–10%)) to give **L2·2TFA** (0.184 g, 0.247 mmol, 84%) as a yellow oil. (Found: C, 54.48; H, 5.46; N, 14.42. $C_{29}H_{37}N_7O_2{\cdot}2(CF_3CO_2H)$ requires C, 53.29; H, 5.30; N, 13.19%); δ_H(300 MHz; CD_3OD; Me_4Si) 1.70 (4H, m, $2CH_2$), 2.12 (3H, s, CH_3), 2.16 (3H, s, CH_3), 2.63 (2H, t, *J* 6.0, CH_2), 2.71 (2H, t, *J* 5.4, CH_2), 2.88 (2H, t, *J* 6.3, CH_2), 3.24 (4H, m, $2CH_2$), 3.61 (2H, t, *J* 6.9 and *J* 7.5, CH_2), 4.00 (2H, t, *J* 5.7 and *J* 6.6, CH_2), 7.61 (2H, t, *J* 4.8 and *J* 6.9, 2CH-Ar), 7.83 (2H, t, *J* 5.1 and *J* 6.9, 2CH-Ar), 8.01 (2H, d, *J* 8.4, 2CH-Ar), 8.13 (2H, d, *J* 8.7, 2CH-Ar). δ_C(75.4 MHz; CD_3OD; Me_4Si) 9.30 (CH_3), 11.56 (CH_3), 27.90 (CH_2), 31.04 (CH_2), 36.66 (CH_2), 40.04 (CH_2), 40.83 (CH_2), 44.88 (CH_2), 45.64 (CH_2), 112.45 ($C_{4\text{-pz}}$), 118.23 (C_{TFA}) 121.44–138.65 (8CH-Ar, 5C-Ar), 140.90 ($C_{3/5\text{-pz}}$), 148.91 ($C_{3/5\text{-pz}}$), 162.94 (C_{TFA}), 173.58 (C=O); δ_F(281.98 MHz; CD_3OD; Me_4Si) –75.81 (CF_3CO_2H); t_R: 10.95 min (100-5 C18, 0.9 ml min^{-1}); *m*/*z* (ESI-MS) 516.1 $[M + H]^+$.

General procedure for the synthesis of the Re complexes (Re1–Re2)

$[Re(H_2O)_3(CO)_3]Br$ was reacted overnight with equimolar amounts of **L1–L2** in refluxing methanol. After this time, the solvent was removed under reduced pressure and the desired products were purified by column chromatography.

***fac*-[Re(CO)$_3$(κ^3-L1)](CF$_3$CO$_2$)$_2$·2TFA. Re1** was obtained by reflux in methanol and purified by column chromatography (eluent: $CHCl_3$ (80–37%)/MeOH (20–45%)/NH_4OH 25% (0–18%)) to give a red–orange solid (90 mg, 0.070 mmol, 68%). (Found: C, 40.77; H, 3.17; N, 9.31. $C_{39}H_{47}F_6N_8O_8Re{\cdot}2(CF_3CO_2H)$ requires C, 40.22; H, 3.85; N, 8.73%); ν_{max}(KBr)/cm^{-1} (CO) 1890, 2024; δ_H(300 MHz; CD_3OD; Me_4Si) 1.84 (2H, m, CH_2), 2.04 (2H, m, CH_2), 2.25 (3H, s, CH_3), 2.32 (3H, s, CH_3), 2.54 (3H, m, 3CH), 2.84 (3H, m, 3CH), 3.33 (12H, s, $4CH_3$), 3.38 (2H, s, CH_2), 3.52 (1H, m, 1CH), 3.86 (1H, s br, 1NH), 4.09 (1H, t, *J* 12.3 and *J* 13.2, 1CH), 4.50 (1H, d, *J* 15.9, 1CH), 4.77 (2H, t, *J* 7.2, CH_2), 5.41 (1H, s br, 1NH), 6.71 (2H, s, 2CH-Ar), 6.91 (1H, s br, 1NH), 7.29 (2H, d, *J* 9.3, 2CH-Ar), 7.93 (2H, d, *J* 9.3, 2CH-Ar), 8.68 (1H, s, CH-Ar); δ_C(75.4 MHz; CD_3OD; Me_4Si) 10.38 (CH_3), 14.57 (CH_3), 24.89 (CH_2), 28.27 (CH_2), 31.30 (CH_2), 40.95 ($4CH_3$), 43.22 (CH_2), 48.72 ($3CH_2$), 55.86 (CH_2), 93.62 (2CH-Ar), 113.98 ($C_{4\text{-pz}}$), 115.52 (2CH-Ar), 118.47 (2C-Ar), 134.37 (2CH-Ar), 143.72 ($C_{3/5\text{-pz}}$), 143.97 (CH-Ar), 144.29 (2C-Ar), 153.46 ($C_{3/5\text{-pz}}$), 157.30 (2C-Ar), 162.93 (TFA), 172.91 (C=O), 194.14-194.71 (3CO); t_R = 17.69 min (100-5 C18, 0.9 ml min^{-1}); *m*/*z* (ESI-MS): 414.9 $[M]^{2+}$.

***fac*-[Re(CO)$_3$(κ^3-L2)](CF$_3$CO$_2$)·2TFA. Re2** was obtained by reflux in methanol and the solvent was removed under reduced pressure to give a yellow solid (49 mg, 0.043 mmol, 89%). (Found: C, 38.04; H, 2.70; N, 8.83. $C_{34}H_{37}F_3N_7O_5Re{\cdot}2(CF_3CO_2H)$ requires C, 38.36; H, 3.49; N, 8.70%); ν_{max}(KBr)/cm^{-1} (CO) 1922, 2024; δ_H(300 MHz; CD_3OD; Me_4Si) 1.75 (2H, m CH_2), 1.81 (2H, m, CH_2), 2.32 (3H, s, CH_3), 2.41 (3H, s, CH_3), 2.51 (1H, m, 1CH), 2.62 (1H, m, 1CH), 2.81 (3H, m, 3CH), 3.43 (3H, m, CH, CH_2), 3.67 (2H, m, CH_2), 3.90 (1H, s br, NH), 4.08 (1H, t, *J* 12.6 and *J* 13.2, 1CH), 4.50 (1H, d, *J* 15.6, 1CH), 5.39 (1H, s br, NH), 6.88 (1H, s br, NH), 7.78 (2H, t, *J* 8.1 and *J* 6.9, 2CH-Ar), 8.05 (2H, t, *J* 6.9 and *J* 7.8, 2CH-Ar), 8.14 (2H, m, 2CH-Ar), 8.26 (2H, d, *J* 8.7, 2CH-Ar); δ_C(75.4 MHz; CD_3OD; Me_4Si) 10.45 (CH_3), 14.58 (CH_3), 27.83 (CH_2), 28.04 (CH_2), 31.34 (CH_2), 40.25 (CH_2), 40.89 (CH_2), 43.26 (CH_2), 55.86 (CH_2), 114.16 ($C_{4\text{-pz}}$), 118.00 (C_{TFA}), 123.78 (2C-Ar), 126.62 (2C-Ar), 127.18 (2CH-Ar), 129.00 (2CH-Ar), 134.77 (2CH-Ar), 143.75 ($C_{3/5\text{-pz}}$), 146.77 (2C-Ar), 147.63 (C-Ar), 153.52 ($C_{3/5\text{-pz}}$), 162.50 (C_{TFA}), 167.96 (C=O), 172.89 (C=O), 194.14-194,63 (3CO); δ_F(281.98 MHz; CD_3OD; Me_4Si) -75.87 (CF_3CO_2H); t_R = 15.06 min (100-5 C18, 0.9 ml min^{-1}); *m*/*z* (ESI-MS): 786.0 $[M]^+$, 393.4 $[M^+ + H]^{2+}$.

General procedure for the synthesis of the ^{99m}Tc complexes (Tc1–Tc2)

In a glass vial, 100 μl of a 10^{-4} M aqueous solution of **L1–L2** were added to 900 μl of the organometallic precursor *fac*-$[^{99m}Tc(CO)_3(H_2O)_3]^+$ (1–2 mCi) in saline at pH 7.4. The reaction

mixture was heated to 100 °C for 30 to 40 min, cooled at room temperature and the final solution analyzed by RP-HPLC.

Partition coefficient measurements

The log $P_{o/w}$ values of complexes **Tc1–Tc2** (Table 1) were determined by the "shake flask" method under physiological conditions (n-octanol/0.1 M PBS, pH 7.4).[16] The HPLC-purified compounds (100 µl, ~100µCi) were added to a test tube containing 1 ml of n-octanol and 1 ml of the PBS solution. The tube was vortexed for 1 min and centrifuged for 5 min at 3500 rpm. After centrifugation, 500 µl of the organic phase were transferred to another tube and further extracted with 500 µl of the PBS solution, as described for the first extraction. After separation of the phases, 50 µl aliquots of each phase were taken for radioactivity measurement (in duplicate) using a γ-counter. The partition coefficient ($P_{o/w}$) was calculated based on the ratio (activity in octanol layer)/(activity in aqueous layer) and is expressed as log $P_{o/w}$.

DNA binding studies

Calf thymus DNA (CT-DNA) sodium salt was purchased from Sigma and was used without further purification. The DNA concentrations per nucleotide of stock solutions in Tris buffer (Tris-HCl 0.1M, pH 7.4) were determined by absorption spectroscopy at 260 nm, after adequate dilution with the buffer and using the reported molar absorptivity of 6600 M^{-1} cm^{-1}.[28] The purity of the DNA samples was checked by monitoring the value A_{260}/A_{280} ratio. All measurements that involved DNA and the different tested compounds (**L1, L2, Re1** and **Re2**) were carried out in Tris buffer (Tris-HCl 0.1M, pH 7.4) or in phosphate buffer (10 mM, pH 7.2).

The absorption and fluorescence titrations were performed by keeping the concentrations of the probe constant, while varying the concentrations of the DNA. To obtain the intrinsic binding constant (K) all calculations were done by considering the DNA concentration in base pairs, and the data were corrected for volume changes.

Absorption spectroscopy studies

UV-Vis absorption spectra were recorded on a Hitachi U-2000 spectrophotometer by using 1 cm path-length quartz cells. In order to eliminate any interference of the DNA absorbance in the region of absorbance of the acridine derivative chromophores an equal amount of CT-DNA in Tris buffer was added to the sample and reference cells. After each addition of CT-DNA, the solution was allowed to equilibrate and the absorption spectrum was recorded until there were no further changes in the absorbance.

According to the Scatchard model[29] the absorption titration data were fitted to eqn (1) where D is the concentration of DNA in base pairs and $\Delta\varepsilon_{ap} = [\varepsilon_a - \varepsilon_F]$ and $\Delta\varepsilon = [\varepsilon_B - \varepsilon_F]$.

$$D/\Delta\varepsilon_{ap} = D/\Delta\varepsilon + 1/\Delta\varepsilon K \quad (1)$$

The apparent extinction coefficient, ε_a, is the ratio of the observed absorbance of the sample and the total concentration of the probe (A_{obs}/[probe]). ε_B and ε_F correspond to the extinction coefficients of the bound and free forms of the probe, respectively. The intrinsic binding constant (K) was determined from the plot of $D/\Delta\varepsilon_{ap}$ *vs.* D.

According to the Kaminoh model[30] the absorption titration data were fitted to eqn (2).

$$A = (A_0 + K[\text{DNA}]A_{sat})/(1 + K[\text{DNA}]) \quad (2)$$

As the concentration of the chromophore and its absorbance in solution (A_0) are known, the value in saturation, A_{sat}, is calculated from the representation of A *vs.* [DNA].

Fluorescence spectroscopy studies

Fluorescence spectra were recorded in a Perkin-Elmer LS50B spectrofluorimeter using a quartz cuvette of 1 cm. After each addition of CT-DNA in Tris buffer, the solution was allowed to equilibrate and the absorption at the excitation wavelength was recorded. The fluorescence spectra were then recorded until there were no further changes in the fluorescence intensity. Compounds **L1** and **Re1** were excited at 470 nm, while compounds **L2** and **Re2** were excited at 359 nm. Emission and excitation slits were chosen in order to maximize the fluorescence intensity. Emission spectra were recorded from $\lambda = 400$–700 nm for compounds **L1** and **Re1**, and from $\lambda = 350$–650 nm for compounds **L2** and **Re2**, with a scan speed of 150 nm min^{-1}. The fluorescence data were also used to determine the intrinsic binding constant (K) of the probes.

According to the Scatchard model[29] the data were fitted to eqn (3) where D is the concentration of DNA in base pairs and $\Delta I_{ap} = [I_{ap} - I_F]$ and $\Delta I = [I_B - I_F]$.

$$D/\Delta I_{ap} = D/\Delta I + 1/\Delta I K \quad (3)$$

The apparent emission intensity, I_a, is the ratio of the observed intensity of the sample and the total concentration of the probe (I_{obs}/[probe]). I_B and I_F correspond to the emission intensities of the bound and free forms of the probe, respectively. The intrinsic binding constant (K) was determined from the plot of $D/\Delta I_{ap}$ *vs.* D.

According to the Kaminoh model[30] the data were fitted to eqn (4).

$$I = (I_0 + K[\text{DNA}]I_{sat})/(1 + K[\text{DNA}]) \quad (4)$$

As the concentration of the chromophore and its emission intensity (I_0) are known, the value in saturation, I_{sat}, is calculated from the representation of I *vs.* [DNA].

According to the McGhee von Hippel model[31] the concentration of the free probe in each sample (C_F) was calculated using eqn (5), where C_T is the total concentration of the probe and P is the ratio of the observed fluorescence intensity of the bound probe to that of the free probe.

$$C_F = C_T(I/I_0 - P)/(1 - P) \quad (5)$$

The value of P is the y-intercept from the plot of I/I_0 *vs.* 1/[DNA], I and I_0 are the fluorescence intensities of the probes in the presence or absence of DNA. The amount of bound probe (C_B) at any concentration is given by $C_T - C_F$. The binding constant (K) and the binding site size (n) in base pairs were obtained from the plot of r/C_F *vs.* r, where $r = C_B/[\text{DNA}]$ using eqn (6).

$$r/C_F = K(1 - nr)[(1 - nr)/[1 - (n - 1)r]]^{n-1} \quad (6)$$

Circular dichroism (CD) studies

The CD spectra were recorded at 24 °C on a Jasco J-720 spectropolarimeter with UV/Vis (200–700 nm) photomultiplier. Solutions of the probe and CT-DNA in Tris buffer were placed in a 1 cm (or 2 cm) path-length quartz cell, and the spectra were recorded in the 200–650 nm region with subtraction of the buffer baseline. The following operating parameters were used to collect the CD spectra: bandwidth, 0.5 nm; sensitivity, 10 mdeg; resolution, 0.2 nm; scan speed, 50 nm min^{-1}; response time 4 s; accumulations, 3.

Linear dichroism (LD) studies

The LD measurements were performed with a Jasco J500 A spectropolarimeter that was equipped with an IBM PC and a Jasco J interface. The studies were done with CT-DNA in 10 mM phosphate buffer at pH 7.2, and the sample orientation was produced by a device that was designed by Wada and Kozawa for the studies of differential flow dichroism of polymer solutions at a shear gradient of 700 rpm.[32] The reduced linear dichroism, was defined by the ratio ($LDr = LD/A_{iso}$) between the LD values and the absorbance of the unoriented sample at rest (A_{iso}), which might be related to the orientation of DNA and the angle between the respective light-absorbing transition moment and DNA helix axis according to Norden *et al.*[33]

Cell studies

Cell culture. B16F1 murine melanoma cells (ECACC, UK) were grown in DMEM containing GlutaMax I supplemented with 10% heat-inactivated fetal bovine serum and 1% penicillin/streptomycin antibiotic solution (all from Invitrogen). Cells were cultured in a humidified atmosphere of 95% air and 5% CO_2 at 37 °C (Heraeus, Germany), with the medium changed every other day.

Fluorescence microscopy

B16F1 murine melanoma cells were cultured overnight on sterile coverslips, at ~5×10^4 cells per well. The next day the medium was discarded and replaced by fresh medium containing the ligands (**L1** or **L2**) or complexes (**Re1** or **Re2**) (70 μM) and cells were incubated for 3 h. After this loading, cells were washed with PBS and fixed for 20 min at room temperature with 3% paraformaldehyde in PBS. After 3 washings with PBS, cells on the coverslips were incubated in 5 μM DAPI (4′-6-diamidino-2-phenylindol) (for **L1** and **Re1**) or 5 μM DRAQ5 (1,5-bis{[2-(dimethylamino)ethyl]amino}-4,8-dihydroxyanthracene-9,10-dione) (for **L2** and **Re2**) for nuclear staining for 20 min at room temperature. After 3 more washings in PBS, the coverslips were mounted on standard microscope slides with glycerol + 3% *N*-propyl gallate to improve the optical conditions and to prevent photobleaching. The samples were then imaged on a Leica DMRA2 upright microscope using a 100× 1.2NA objective and a Chroma +A4 UV filter for evaluating the fluorescence of DAPI (λ_{ex} max= 359 nm, λ_{em} max= 461 nm) and **L2** and **Re2**, a Y5 Cy5 filter for DRAQ5 (λ_{ex} max= 647 nm, λ_{em} max= 670 nm) and a L5 FITC filter for **L1** and **Re1**. Images were acquired and colour-combined by using a CoolSNAP HQ 1.3 Mpixel-cooled CCD camera and the MetaMorph software.

Confocal fluorescence microscopy

B16F1 murine melanoma cells were prepared as described above and incubated with **L1** and **Re1** (70 μM) and 5 μM DAPI solution for nuclear staining. After washing, the coverslips were mounted on standard microscope slides. The samples were then imaged on a Zeiss LSM 510 META inverted laser scanning confocal microscope using a 63×/1.4 Apochromat objective. The fluorescence of **L1** and **Re1** was detected using the 488 nm laser line of an Argon/2 laser and a BP 505-550 emission filter. DAPI fluorescence was detected using a 405 nm Diode laser and a BP 420-480 emission filter.

Cellular internalization and retention

The cellular internalization assay was performed in B16F1 murine melanoma cells seeded at a density of 2×10^5 cells per well in 24-well tissue culture plates and allowed to attach overnight. The cells were incubated at 37 °C for a period of 5 min to 24 h with about 200 000 cpm of the complex in 0.5 mL of assay medium [MEM with 25 mM *N*-(2-hydroxyethyl)piperazine-*N*′-ethanesulfonic acid and 0.2% BSA]. Incubation was terminated by washing the cells with ice-cold assay medium. Cell-surface-bound radioligand was removed by two steps of acid wash (50 mM glycine·HCl/100 mM NaCl, pH 2.8) at room temperature for 5 min. pH was neutralized with cold PBS with 0.2% BSA and, subsequently, the cells were lysed by a 10 min incubation with 1 N NaOH at 37 °C to determine the internalized radioligand. The cellular retention of the internalized radioconjugate was determined by incubating cells with the radiolabeled compound for 3 h at 37 °C, washing them with cold assay medium, removing the membrane-bound radioactivity with acid buffer wash and monitoring radioactivity release into the culture media (0.5 ml) at 37 °C. At different time points over a 4 h incubation period, the radioactivity in the medium and in the cells were separately collected and counted in a γ-counter. Cellular internalization and retention data was based on three determinations for each time point, and are expressed as an average plus the standard deviation.

Nuclear internalization

B16F1 cells were seeded at a density of 0.2 million/well into 24-well tissue culture plates and allowed to attach overnight. Cells were incubated in humidified 5% CO_2/95% air, 37 °C for a period of 30 min, 1, 2, 3, 4, 5 and 6 h with about 200 000 cpm of radioconjugate in 0.5 mL of assay medium. After incubation cells were washed with PBS with 0.2% BSA (250μl/well) and removed from the plate with trypsin (100 μl/well). The inactivation of trypsin was performed with 250 μl of culture medium. The cells in suspension were centrifuged (800 rpm, 2 min) and washed twice with cold PBS with 0.2% BSA. Cells were lysed in 500 μl of lysis buffer (Tris 10 mM, $MgCl_2$ 1.5 mM, NaCl 140 mM, Nonidet P-40 0.02%, pH 8.0–8.3). After 15 min of incubation in ice, the cell suspension was centrifuged at 1300 *g* at 4 °C for 1 min. The activities of supernatant (activity outside the nucleus) and of the precipitate (activity retained in the nucleus) were measured (3 replicates) in a γ-counter for different incubation times.

Plasmid DNA studies

DNA cleavage activity was evaluated by monitoring the conversion of supercoiled plasmid DNA (sc) to open circular DNA (oc) or linear DNA. Plasmid DNA (300 ng, pUC19) was incubated with complexes **Re1** and **Tc1** for 48 h at room temperature in Tris (pH = 7.4). After this time, 5 μL of DNA loading buffer was added and the samples were loaded onto a 0.8% agarose gel (AppliChem) in TBE 1× (Tris-borate-EDTA) buffer containing 15 μL of ethidium bromide (10 mg mL^{-1}, AppliChem) for visualization of DNA. Controls of non-incubated and of linearized plasmid were included in both extremes of an 18-well gel plate. The electrophoresis was carried out for 18 h at 20 mV. Bands were visualised under UV light and photographed using an AlphaImager EP (Alpha Innotech). All samples in the figure were obtained from the same run. Peak areas were measured by densiometry using AlphaView Software from Alpha Innotech. Peak areas for the sc form were corrected using the factor 1.42 to account for its lower staining capacity by ethidium bromide[34] and used to calculate the percentage of each form (sc and oc), and the ratio sc/oc.

Acknowledgements

Teresa Esteves and Sofia Gama thank the FCT for a doctoral and postdoctoral research grants (SFRH/BD/29154/2006 and SFRH/BPD/29564/2006, respectively). COST Action D39 is also acknowledge. The QITMS instrument was acquired with the support of the Programa Nacional de Reequipamento Científico (Contract>REDE/1503/REM/2005-ITN) of Fundação para a Ciência e a Tecnologia and is part of RNEM - Rede Nacional de Espectrometria de Massa.

References

1 J. Carlsson, T. Stigbrand and G. P. Adams, in *Targeted Radionuclide Tumor Therapy*, ed. Carlsson, T. Stigbrand and G. P. Adams, Springer Science, 1st edn, 2008, ch. 1, pp. 1–11.
2 A. M. Scott and S-T. Lee, in *Targeted Radionuclide Tumor Therapy*, ed. Carlsson, T. Stigbrand and G. P. Adams, Springer Science, 1st edn, 2008, ch. 20, pp. 349–385.
3 K. G. Hofer, *Acta Oncol.*, 2000, **39**, 687–692.
4 V. N. Karamychev, M. W. Reed, R. D. Neuman and I. G. Panyutin, *Acta Oncol.*, 2000, **39**, 687–692.
5 F. Buchegger, F. P.- Adamer, Y. M. Dupertuid and A. B. Delaloye, *Eur. J. Nucl. Med. Mol. Imaging*, 2006, **33**, 1352–1363.
6 M. Ginj, K. Hinni, S. Tschumi, S. Schulz and H. R. Maecke, *J. Nucl. Med.*, 2005, **46**, 2097–2103.
7 Z. Cai1, J.-P. Pignol, C. Chan and R. M. Reilly, *J. Nucl. Med.*, 2010, **51**, 462–470.
8 P. Häfliger, N. Agorastos, B. Spingler, O. Georgiev, G. Viola and R. Alberto, *ChemBioChem*, 2005, **6**, 414–421.
9 M. Ginj and H. R. Maecke, *Tetrahedron Lett.*, 2005, **46**, 2821–2824.
10 F. Marques, A. Paulo, M. P. Campello, S. Lacerda, R. F. Vitor, L. Gano, R. Delgado and I. Santos, *Radiat. Prot. Dosim.*, 2005, **116**, 601–604.
11 R. F. Vitor, M. Videira, F. Marques, A. Paulo, J. C. Pessoa, G. Viola, G. G. Martins and I. Santos, *ChemBioChem*, 2008, **9**, 131–142.
12 R. F. Vitor, T. Esteves, F. Marques, P. Raposinho, A. Paulo, S. Rodrigues, J. Rueff, S. Casimiro, L. Costa and I. Santos, *Cancer Biother. Radiopharm.*, 2009, **24**, 551–563.
13 N. Agorastos, L. Borsig, A. Renard, P. Antoni, G. Viola, B. Spingler, P. Kurz and R. Alberto, *Chem.–Eur. J.*, 2007, **13**, 3842–3852.
14 C. Moura, T. Esteves, L. Gano, P. D. Raposinho, A. Paulo and I. Santos, *New J. Chem.*, **2010**, DOI: 10.1039/c0nj00256a.
15 S. Alves, A. Paulo, J. D. G. Correia, A. Domingos and I. Santos, *J. Chem. Soc., Dalton Trans.*, 2002, 4714–4719.
16 D. E. Troutner, W. A. Volkert, T. J. Hoffman and R. A. Holmes, *Int. J. Appl. Radiat. Isot.*, 1984, **35**, 467–470.
17 E. Fredericq and C. Houssier, *Biopolymers*, 1972, **11**, 2281–2308.
18 F. Zimmermann, B. Hossenfelder, J-C. Panitz and A. Wokaun, *J. Phys. Chem.*, 1994, **98**, 12796–12804.
19 B. E. Bowler, K. J. Ahmed, W. I. Sundquist, L. S. Hollis, E. E. Whang and S. J. Lippard, *J. Am. Chem. Soc.*, 1989, **111**, 1299–1306.
20 Elizabeth Kuruvilla, Paramjyothi C. Nandajan, Gary B. Schuster and Danaboyina Ramaiah, *Org. Lett.*, 2008, **10**, 4295–4298.
21 M. B. Lyles and I. L. Cameron, *Biophys. Chem.*, 2002, **96**, 53.
22 N. Kure, T. Sano, S. Harada and T. Yasunaga, *Bull. Chem. Soc. Jpn.*, 1988, **61**, 643.
23 J. Kapuscinski and Z. Darzynkiewicz, *J. Biomol. Struct. Dyn.*, 1987, **5**, 127.
24 A. Rodger, S. Taylor, G. Adlam, I. S. Blagbrough and I. S. Haworth, *Bioorg. Med. Chem.*, 1995, **3**, 861–872.
25 D. D. Perrin, and W. L. Armarego, *Purification of Laboratory Chemicals*, Pergamon Press, Oxford, 3rd edition, 1988.
26 A. Drews, H.-J. Pietzsch, R. Syhre, S. Seifert, K. Varnäs, H. Hall, C. Halldin, W. Kraus, P. Karlsson, C. Johnson, H. Spies and B. Johannsen, *Nucl. Med. Biol.*, 2002, **29**, 389–398.
27 N. Lazarova, S. James, J. Babich and J. Zubieta, *Inorg. Chem. Commun.*, 2004, **7**, 1023–1026.
28 C. V. Kumar and E. H. Asuncion, *J. Am. Chem. Soc.*, 1993, **115**, 8547–8553.
29 C. V. Kumar, E. H. A. Punzalan and W. B. Tan, *Tetrahedron*, 2000, **56**, 7027–7040.
30 N. C. Santos, M. Prieto and M. A. R. B. Castanho, *Biochim. Biophys. Acta*, 2003, **1612**, 123–135.
31 J. McGhee and P. von Hippel, *J. Mol. Biol.*, 1974, **86**, 469–489.
32 A. Wada and S. Kozawa, *J. Polym. Sci. Part A*, 1964, **2**, 853–864.
33 B. Norden, M. Kubista and T. Kurucsev, *Q. Rev. Biophys.*, 1992, **25**, 51–170.
34 R. S. Lloyd, C. W. Haidle and D. L. Robberson, *Biochemistry*, 1978, **17**, 1890–1896.

